Design, Implementation and Evaluation of Parallel Pipelined STAP on Parallel Computers

Alok Choudhary

Wei-keng Liao
Donald Weiner
Pramod Varshney

Richard Linderman[†]
Mark Linderman[†]
Russell Brown[‡]

ECE Department
Northwestern University
Evanston, IL 60208

EECS Department
Syracuse University
Syracuse, NY 13244

Information Directorate[†]
Sensors Directorate[‡]
Air Force Research Laboratory

Abstract

This paper presents performance results for the design and implementation of parallel pipelined Space-Time Adaptive Processing (STAP) algorithms on parallel computers. In particular, the paper describes the issues involved in parallelization, our approach to parallelization and performance results on an Intel Paragon. The paper also discusses the process of developing software for such an application on parallel computers when latency and throughput are both considered together and presents tradeoffs considered with respect to inter and intra-task communication and data redistribution. The results show that not only scalable performance was achieved for individual component tasks of STAP but linear speedups were obtained for the integrated task performance, both for latency as well as throughput. Results are presented for up to 236 compute nodes (limited by the machine size available to us). Another interesting observation made from the implementation results is that performance improvement due to the assignment of additional processors to one task can improve the performance of other tasks without any increase in the number of processors assigned to them. Normally, this cannot be predicted by theoretical analysis.

1 Introduction

Space-time adaptive processing (STAP) is a well known technique in the area of airborne surveillance radars used to detect weak target returns embedded in strong ground clutter, interference, and receiver noise. STAP is a 2-dimensional adaptive filtering algorithm that attenuates unwanted signals by placing nulls in their directions of arrival and Doppler frequencies. Most STAP applications are computationally intensive and must operate in real time. High performance computers are becoming mainstream due to the progress made in hardware as well as software support in the last few years. They can satisfy the STAP computational requirements of real-time applications while increasing the flexibility, affordability, and scalability of radar signal processing systems. However, efficient parallelization of a STAP algorithm which has embedded in it different processing steps is challenging and is the subject of this paper.

This paper describes our innovative parallel pipelined implementation of a Pulse Repetition Interval (PRI)-staggered post-Doppler STAP algorithm on the Intel Paragon at the Air Force Research Laboratory (AFRL), Rome, New York. For a detailed description of the STAP algorithm implemented in this work, the reader is referred to [1, 2]. AFRL successfully installed their implementation of the STAP algorithm onboard an airborne platform and performed four flight experiments in May and June 1996 [3]. These experiments were performed as part of the Real-Time Multi-Channel Airborne Radar Measurements (RTMCARM) program. The RTMCARM system block diagram is shown in Figure 1. In that real-time demonstration, live data from a phased array radar was processed by the onboard Intel Paragon and results showed that high performance computers can deliver a significant performance gain. However, this implementation used compute nodes of the machine only as independent resources in a round robin fashion to run different instances of STAP (rather than speeding up each instance of STAP.) Using this approach, the throughput may be improved, but the latency is limited by what can be achieved using one compute node.

Parallel computers, organized with a large set (several hundreds) of processors linked by a specialized high speed interconnection network, offer an attractive solution to many computationally intensive applications, such as image processing, simulation of particle reactions, and so forth. Parallel processing splits an application problem into several subproblems which are solved on

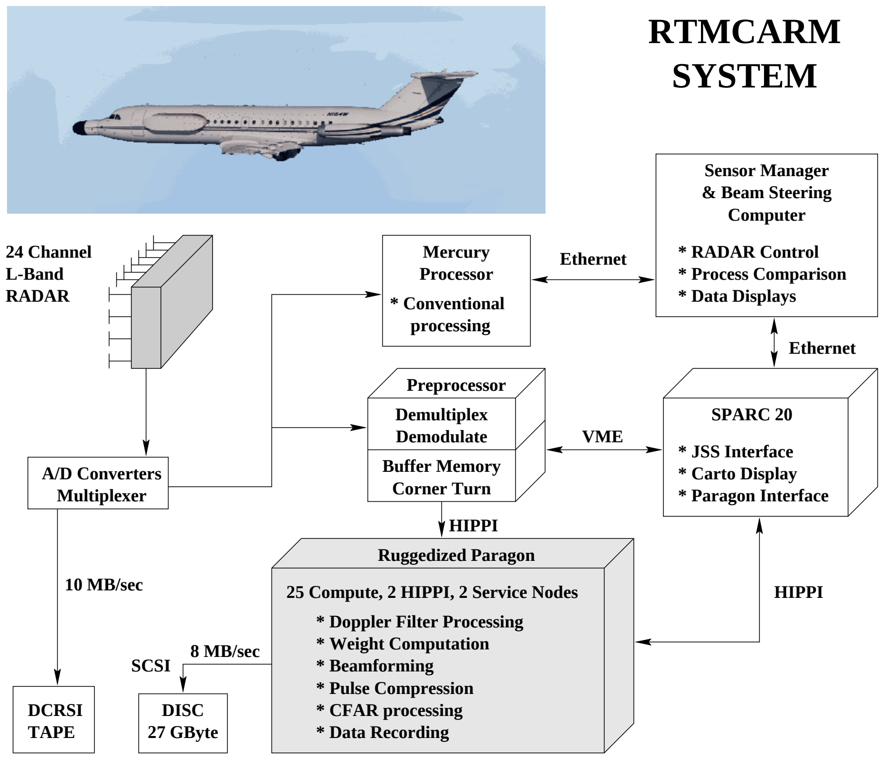

Figure 1. RTMCARM system block diagram.

multiple processors simultaneously. To learn more about parallel computing, the reader is referred to [4, 5, 6, 7, 8]. For our parallel implementation of this real application we have designed a model of the parallel pipeline system where each pipeline is a collection of tasks and each task itself is parallelized. This parallel pipeline model was applied to the STAP algorithm with each step as a task in a pipeline. This permits us to significantly improve latency as well as throughput.

This paper discusses both the parallelization process and performance results. In addition, design considerations for portability, task mapping, parallel data redistribution, parallel pipelining as well as system-level and task-level performance measurement are presented. Finally, the performance and scalability of the implementation for a large number of processors is demonstrated. Performance results are given for the Intel Paragon at AFRL.

The paper is organized as follows. In Section 2 we discuss the related work. An overview of the implemented algorithm is given in Section 3. In Section 4 we present the parallel pipeline system model and discuss some parallelization issues and approaches for implementation of STAP algorithms. Section 5 presents specific details of STAP implementation. Performance results and

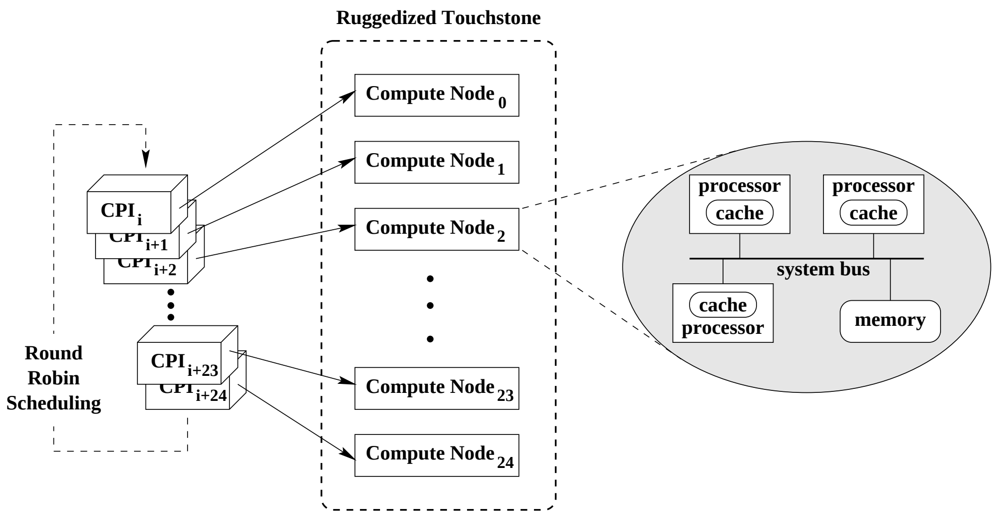

Figure 2. Implementation of the ruggedized version of Intel Paragon system in RTMCARM experiments.

conclusions are presented in Section 7 and Section 8, respectively.

2 Related Work

The RTMCARM experiments were performed using a BAC 1-11 aircraft. The radar was a phased array L-Band radar with 32 elements organized into two rows of 16 each. Only the data from the upper 16 elements were processed with STAP. This data was derived from a 1.25 MHz intermediate frequency (IF) signal that was 4:1 oversampled at 5 MHz. The number representation at IF was 14 bits, 2's complement and was converted to 16 bit baseband real and imaginary numbers. Special interface boards were used to digitally demodulate IF signals to baseband. The signal data formed a raw 3-dimensional data cube, called the coherent processing interval (CPI) data cube, comprised of 128 pulses, 512 range gates (32.8 miles), and 16 channels. These special interface boards were also used to corner turn the data cube so that the CPI is unit stride along pulses. This speeds the subsequent Doppler processing on the High Performance Computing (HPC) systems. Live CPI data from a phased-array radar were processed by a ruggedized version of the Paragon computer.

The ruggedized version of the Intel Paragon system used for the RTMCARM experiments consists of 25 compute nodes running the SUNMOS operating system. Figure 2 depicts the system implementation. Each compute node has three i860 processors accessing the common memory of size 64M bytes as a shared resource. The CPI data sets were sent to the 25 compute nodes in a round robin manner and all three processors worked on each CPI data set as a shared-memory machine. The system processed up to 10 CPIs per second (throughput) and achieved a latency of 2.35 seconds per CPI. This implementation used compute nodes of the machine as independent resources to run different instances of CPI data sets. No communication among compute nodes was needed. This approach can achieve desired throughput by using as many nodes as needed, but the latency is limited by what can be achieved using the three processors in one compute node. More information on the overall system configuration and performance results can be found in [1, 3].

Other related work [9, 10, 11, 12] parallelized high-order post-Doppler STAP algorithms by partitioning the computational workload among all processors allocated for the applications. In [9, 10], the work focused on the design of parallel versions of subroutines for FFT and QR decomposition. In [11, 12], the implementations optimized the data redistribution between processing steps in the STAP algorithms while using sequential versions of the FFT and QR decomposition subroutines. A multi-stage approach was employed in [13] which was an extension of [11, 12]. A beam space post-Doppler STAP was divided into three stages and each stage was parallelized on a group of processors. A technique called replication of pipeline stages was used to replicate the computational intensive stages such that a different data instance is run on a different replicated stage. Their effort focused on increasing the throughput while keeping the latency fixed. For other related work, the reader is referred to [14, 15, 16].

3 Algorithm Overview

The adaptive algorithm, which cancels Doppler shifted clutter returns as seen by the airborne radar system, is based on a least squares solution to the weight vector problem. This approach has traditionally yielded high clutter rejection but suffers from severe distortions in the adapted main beam pattern and resulting loss of gain on the target. Our approach, which is described in greater detail in the Appendix, introduces a set of constraint equations into the least squares problem which can be weighted proportionally to preserve main beam shape. The algorithm is structured so that multiple receive beams may be formed without changing the matrix of training data. Thus, the adaptive problem can be solved once for all beams which lie within the transmit illumination region. The airborne radar system was programmed to transmit five beams, each 25 degrees in width, spaced 20 degrees apart. Within each transmit beam, six receive beams were formed by the processor.

A MATLAB version of the code which was parallelized is presented in the Appendix. The algorithm consists of the following steps:

1. Doppler filter processing,
2. Weight computation,
3. Beamforming,
4. Pulse compression, and
5. CFAR processing.

Doppler filtering is performed on each receive channel using weighted Fast Fourier Transforms (FFT's). The analog portion of the receiver compensates the received clutter frequency to center the clutter frequency at zero regardless of the transmit beam position. This simplifies indexing of Doppler bins for classification as ”easy” or ”hard” depending on their proximity to mainbeam clutter returns. For the hard cases, Doppler processing is performed on two 125-pulse windows of data separated by three pulses (a STAP technique known as ”PRI-stagger”). Both sets of Doppler processed data are adaptively weighted in the beamforming process for improved clutter rejection. In the easy case, only a single Doppler spectrum is computed. This simpler technique has been termed Post Doppler Adaptive Beamforming and is quite effective at a fraction of the computational cost when the Doppler bin is well separated from mainbeam clutter. In these situations, an angular null placed in the direction of the competing ground clutter provides excellent rejection. Selectable window functions are applied to the data prior to the Doppler FFT's to control sidelobe levels. The selection of a window is a key parameter in that it impacts the leakage of clutter returns across Doppler bins, traded off against the width of the clutter passband.

An efficient method of beamforming using recursive weight updates is made possible by a block update form of the QR decomposition algorithm. This is especially significant in the hard Doppler regions, which are computed using separate weights for six consecutive range intervals. The recursive algorithm requires substantially less training data (sample support) for accurate weight computation, as well as providing improved efficiency. Since the hard regions have one sixth the range extent from which to draw data, this approach dealt with the paucity of data by using past looks at the same azimuth, exponentially forgotten, as independent, identically distributed estimates of the clutter to be cancelled. This assumes a reasonable revisit time for each azimuth beam position. During the flight experiments, the five 25 degree transmit beam positions were revisited at a 1-2 Hz rate (5-10 CPIs per second.)

The training data for the easy Doppler regions was selected using a more traditional approach. Here, the entire range extent was available for sample support, so the entire training set was drawn from three preceding CPIs for application to the next CPI in this azimuth beam position. In this case, a regular (non-recursive) QR decomposition is performed on the training data, followed by block update to add in the beam shape constraints.

Pulse compression is a compute intensive task, especially if applied to each receive channel independently. In general, this approach is required for adaptive algorithms which compute different weight sets as a function of radar range. Our algorithm, however, with its mainbeam constraint, preserves phase across range. In fact, the phase of the solution is independent of the clutter nulling equations, and appears only in the constraint equations. The adapted target phase is preserved across range, even though the clutter and adaptive weights may vary with range. Thus, pulse compression may be performed on the beamformed output of the receive channels providing a substantial savings in computations.

In the sections to follow, we present the process of parallelization and software design considerations including those for portability, task mapping, parallel data redistribution, parallel pipelining and issues involved in measuring performance in implementations when not only the performance of individual tasks is important, but overall performance of the integrated system is critical. We demonstrate the performance and scalability for a large number of processors.

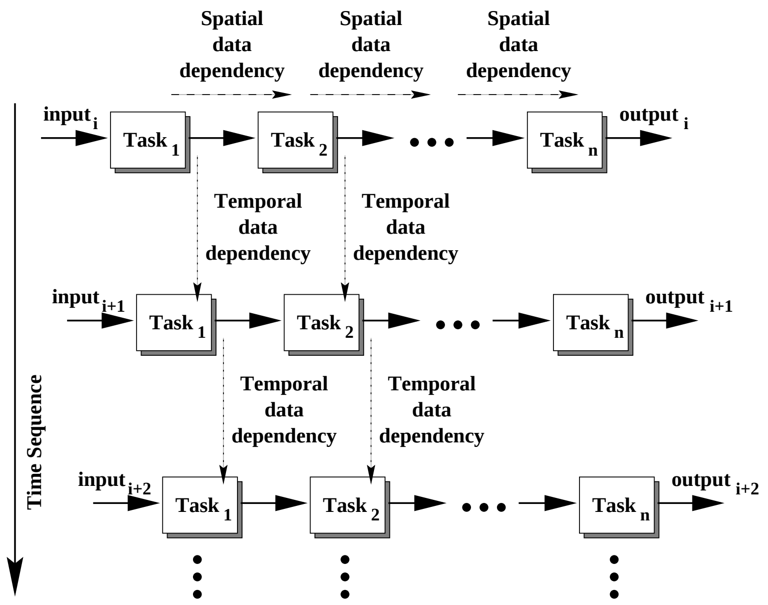

Figure 3. Model of the parallel pipeline system. (Note that $Task_i$ for all input instances is executed on the same number of processors, but that the number of processors may differ from one task to another.)

4 Model of the Parallel Pipelined System

The system model for the type of STAP applications considered in this work is shown in Figure 3. A pipeline is a collection of tasks which are executed sequentially. The input to the first task is obtained normally from sensors or other input devices with the inputs to the remaining tasks coming from outputs of previous tasks. The set of pipelines shown in the figure indicates that the same pipeline is repeated on subsequent input data sets. Each block in a pipeline represents one task, that is parallelized on multiple (different number of) processors. That is, each task is decomposed into subtasks to be performed in parallel. Therefore, each pipeline is a collection of parallel tasks.

In such a system, there exist both spatial and temporal parallelism that result in two types of data dependencies and flows, namely, spatial data dependency and temporal data dependency [17, 18, 19]. Spatial data dependency can be classified into inter-task data dependency and intra-task data dependency. Intra-task data dependencies arise when a set of subtasks needs to exchange intermediate results during the execution of a parallel task in a pipeline. Inter-task data dependency is due to the transfer and reorganization of data passed onto the next parallel task in the pipeline. Inter-task communication can be communication from the subtasks of the current task to the subtasks of the next task, or collection and reorganization of output data of the current task and then redistribution of the data to the next task. The choice depends on the underlying architecture, mapping of algorithms and input-output relationship between consecutive tasks. Temporal data dependency occurs when some form of output generated by the tasks executed on the previous data set are needed by tasks executing the current data set. STAP is an interesting parallelization problem because it exhibits both types of data dependency.

4.1 Parallelization Issues and Approaches

A STAP algorithm involves multiple algorithms (or processing steps), each of which performs particular functions, to be executed in a pipelined fashion. Multiple pipelines need to be executed in a staggered manner to satisfy the throughput requirements. Each task needs to be parallelized for the required performance, which, in turn, requires addressing the issue of data distribution on the subset of processors on which a task is parallelized to obtain good efficiency and incur minimal communication overhead. Given that each task is parallelized, data flow among multiple processors of two or more tasks is required and, therefore, communication scheduling techniques become critical.

4.1.1 Inter-task Data Redistribution

In an integrated system, data redistribution is required to feed data from one parallel task to another, because the way data is distributed in one task may not be the most appropriate distribution for the next task for algorithmic or efficiency reasons. For example, the FFTs in the Doppler filter processing task perform optimally when the data is unit-stride in pulse, while the next stage, beamforming, performs optimally when the data is unit stride in channel. To ensure efficiency and continuity of memory access, data reorganization and redistribution are required in the inter-task communication phase. Data redistribution also allows concentration of communication at the beginning and the end of each task.

We have developed runtime functions and strategies that perform efficient data redistribution

[20]. These techniques reduce the communication time by minimizing contention on the communication links as well as by minimizing the overhead of processing for redistribution (which adds to the latency of sending messages). We take advantage of lessons learned from these techniques to implement the parallel pipelined STAP application.

4.1.2 Task Scheduling and Processor Assignment

An important factor in the performance of a parallel system is how the computational load is mapped onto the processors in the system. Ideally, to achieve maximum parallelism, the load must be evenly distributed across the processors. The problem of statically mapping the workload of a parallel algorithm to processors in a distributed memory system has been studied under different problem models, such as [21, 22]. The mapping policies are adequate when an application consists of a single task, and the computational load can be determined statically. These static mapping policies do not model applications consisting of a sequence of tasks (algorithms) where the output of one task becomes the input to the next task in the sequence.

Optimal use of resources is particularly important in high-performance embedded applications due to limited resources and other constraints such as desired latency or throughput [23]. When several parallel tasks need to be executed in a pipelined fashion, tradeoffs exist between assigning processors to maximize the overall throughput and assigning processors to minimize a single data set's response time (or latency.) The throughput requirement says that when allocating processors to tasks, it should be guaranteed that all the input data sets will be handled in a timely manner. That is, the processing rate should not fall behind the input data rate. The response time criteria, on the other hand, require minimizing the latency of computation on a particular set of data input.

To reduce the latency, each parallel task must be allocated more processors to reduce its execution time, and consequently, the overall execution time of the integrated system. But it is well known that the efficiency of parallel programs usually decreases as the number of processors is increased. Therefore, the gains in this approach may be incremental. On the other hand, throughput can be increased by increasing the latency of individual tasks by assigning them fewer processors and, therefore, increasing efficiency, but at the same time having multiple streams active concurrently in a staggered manner to satisfy the input-data rate requirements. We next present these tradeoffs and discuss various implementation issues.

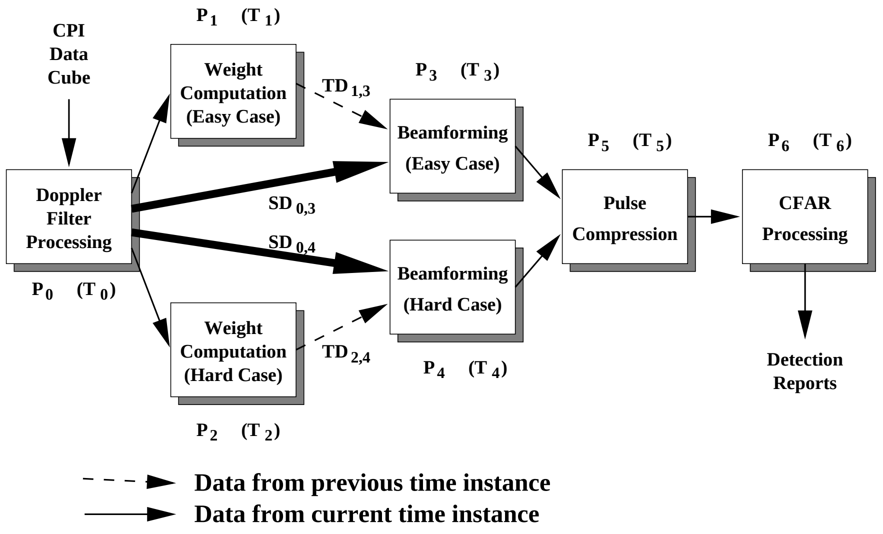

Figure 4. Implementation of parallel pipelined STAP. Arrows connecting task blocks represent data transfer between tasks.

5 Design and Implementation

The design of the parallel pipelined STAP algorithm is shown in Figure 4. The parallel pipeline system consists of seven basic tasks. We refer to the parallel pipeline as simply a pipeline in the rest of this paper. The input data set for the pipeline is obtained from a phased array radar and is formed in terms of a coherent processing interval (CPI). Each CPI data set is a 3-dimensional complex data cube comprised of K range cells, J channels, and N pulses. The output of the pipeline is a report on the detection of possible targets. The arrows shown in Figure 4 indicate data transfer between tasks. Although a single arrow is shown, note that each represents multiple processors in one task communicating with multiple processors in another task. Each task i is parallelized by evenly partitioning its work load among P_i processors. The execution time associated with task i, T_i, consists of the time to receive data from the previous task, computation time, and time to send results to the next task.

The calculation of weights is the most computationally intensive part of the STAP algorithm. For the computation of the weight vectors for the current CPI data cube, data cubes from previous CPIs are used as input data. This introduces temporal data dependency. For example, suppose that a set of CPI data cubes entering the pipeline sequentially are denoted by CPI_i, $i = 0, 1, \ldots$.

At any time instance i, the Doppler filtering task is processing CPI_i and the beamforming task is processing CPI_{i-1}. In the meanwhile, the weight computation task is using past CPIs in the same azimuthal direction to calculate the weight vectors for CPI_i as described below. The computed weight vectors will be applied to CPI_i in the beamforming task at the next time instance ($i+1$). Thus, temporal data dependencies exist and are represented by arrows with dashed lines, $TD_{1,3}$ and $TD_{2,4}$, in Figure 4 where $TD_{i,j}$ represents temporal data dependency of task j on data from task i. In a similar manner, spatial data dependencies $SD_{i,j}$ can be defined and are indicated in Figure 4 by arrows with solid lines.

Throughput and latency are two important measures for performance evaluation on a pipeline system. The throughput of our pipeline system is the inverse of the maximum execution time among all tasks, i.e.,

$$throughput = \frac{1}{\max\limits_{0 \le i < 7} T_i}. \tag{1}$$

To maximize the throughput, the maximum value of T_i should be minimized. In other words, no task should have an extremely large execution time. With a limited number of processors, the processor assignment to different tasks must be made in such a way that the execution time of the task with highest computation time is reduced.

The latency of this pipeline system is the time between the arrival of the CPI data cube at the system input and the time at which the detection report is available at the system output. Therefore, the latency for processing one CPI is the sum of the execution times of all the tasks except weight computation tasks, i.e.,

$$latency = T_0 + max(T_3, T_4) + T_5 + T_6. \tag{2}$$

Equation (2) does not contain T_1 and T_2. The temporal data dependency does not affect the latency because weight computation tasks use data from the previous instance of CPI data rather than the current CPI. The filtered CPI data cube sent to the beamforming tasks do not wait for the completion of its weight computation but rather for the completion of the weight computation of the previous CPI. For example, when the Doppler filter processing task is processing CPI_i, the weight computation tasks use the filtered CPI data, CPI_{i-1}, to calculate the weight vectors for CPI_i. At the same time, the beamforming tasks are working on CPI_{i-1} using the data received from the Doppler filter processing and weight computation tasks. The beamforming tasks do not wait for the completion of the weight computation task when processing CPI_{i-1} data. The overall system latency can be reduced by reducing the execution times of the parallel tasks, e.g., T_0, T_3, T_4, T_5, and T_6 in our system.

Next, we briefly describe each task and its parallel implementation. A detailed description of the STAP algorithm we used can be found in [1, 2].

5.1 Doppler Filter Processing

The input to the Doppler filter processing task is one CPI complex data cube received from a phased array radar. The computation in this task involves performing range correction for each range cell and the application of a windowing function (e.g. Hanning or Hamming) followed by a N-point FFT for every range cell and channel. The output of the Doppler filter processing task is a 3-dimensional complex data cube of size $K \times 2J \times N$ which is referred to as staggered CPI data. In Figure 4, we can see that this output is sent to the weight computation task as well as to the beamforming task.

Both the weight computation and the beamforming tasks are divided into easy and hard parts. These two parts use different portions of staggered CPI data and the associated amounts of computation are also different. The easy weight computation task uses range samples only from the first half of the staggered CPI data while the hard weight computation task uses range samples from the entire staggered CPI data. On the other hand, easy and hard beamforming tasks use all range cells rather than some of them. Therefore, the size of data to be transfered to the weight computation tasks is different from the size of data to be sent to the beamforming tasks. In Figure 4, thicker arrows connected from the Doppler filter processing task to the beamforming tasks indicates that the amount of data sent to the beamforming tasks is more than the amount of data sent to the weight tasks.

The basic parallelization technique employed in the Doppler filtering processing task is to partition the CPI data cube across the range cells, that is, if P_0 processors are allocated to this task, then each processor is responsible for $\frac{K}{P_0}$ range cells. The reason for partitioning the CPI data cube along dimension K is that it maintains an efficient accessing mechanism for contiguous memory space. A total of $K \cdot 2J$ N-point FFTs are performed and the best performance is achieved when

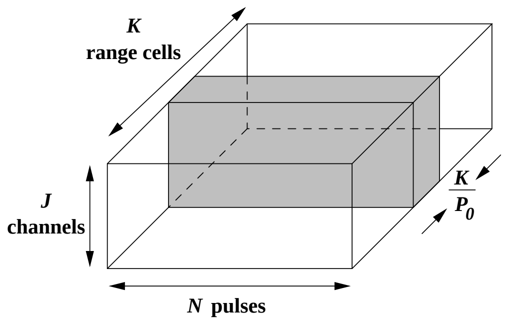

Figure 5. Partitioning strategy for Doppler filter processing task. The CPI data cube is partitioned among P_0 processors across dimension K.

every N-point FFT accesses its N data sets from a contiguous memory space. Figure 5 illustrates the parallelization of this step. The inter-task communication from the Doppler filter processing task to weight computation tasks is explained in Figure 6(b). Since only subsets of range cells are needed in weight computation tasks, data collection has to be performed on the output data before passing it to the next tasks. Data collection is performed to avoid sending redundant data and hence reduces the communication costs.

5.2 Weight Computation

The second step in this pipeline is the computation of weights that will be applied to the next CPI. This computation for N pulses is divided into two parts, namely, ”easy” and ”hard” Doppler bins, as shown in Figure 6(a). The hard Doppler bins (pulses), N_{hard}, are those in which significant ground clutter is expected. The remaining bins are easy Doppler bins, N_{easy}. The main difference between the two is the amount of data used and the amount of computation required. Not all range cells in the staggered CPI are used in weight calculation and different subsets of range samples are used in easy Doppler bins and hard Doppler bins.

To gather range samples for easy Doppler bins to calculate the weight vectors for the current CPI, data is drawn from three preceding CPIs by evenly spacing out over the first one third of K range cells of each of the three CPIs. The easy weight computation task involves N_{easy} QR factorizations, block updates, and back substitutions. In the easy weight calculation, only range samples in the first half of the staggered CPI data are used while hard weight computation employs range samples

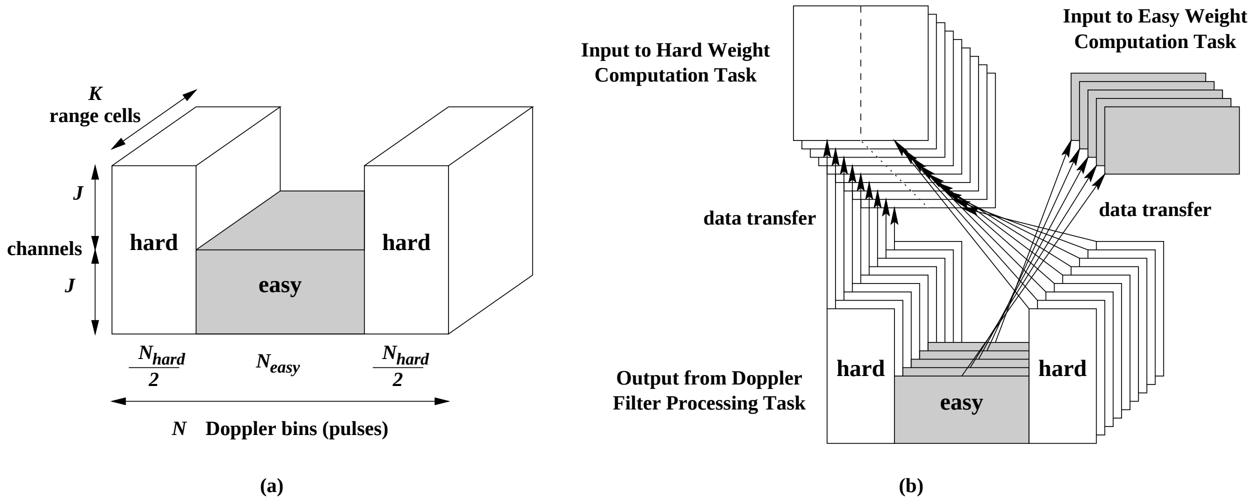

Figure 6. (a) Staggered CPI data partitioned into easy and hard weight computation tasks. (b) Parallel inter-task communication from Doppler filter processing task to easy and hard weight computation tasks requires different sets of range samples. Data collection needs to be performed before the communication. This can be viewed as irregular data redistribution.

from the entire staggered CPI. Furthermore, the range extent for hard Doppler bins is split into six independent segments to further improve clutter cancelation. To calculate weight vectors for the current CPI, the range samples used in hard Doppler bins are taken from the immediately preceding staggered CPI combined with older, exponentially forgotten, data from CPIs in the same direction. This is done for each of the six range segments. The hard weight computation task involves $6N_{hard}$ recursive QR updates, block updates, and back substitutions. The easy and hard weight computation tasks process sets of 2-dimensional matrices of different sizes.

Temporal data dependency exists in the weight computation task because both easy and hard Doppler bins use data from previous CPIs to compute the weights for the current CPI. The outputs of this step, the weight vectors, are two 3-dimensional complex data cubes of size $N_{easy} \times J \times M$ and $N_{hard} \times 2J \times M$ for the easy and hard weight computation tasks, respectively, where M is the number of receive beams. These two weight vectors are to be applied to the current CPI in the beamforming task. Because of the different sizes of easy and hard weight vectors, the beamforming task is also divided into easy and hard parts to handle different amounts of computation.

Given the uneven nature of the weight computations, different sets of processors are allocated

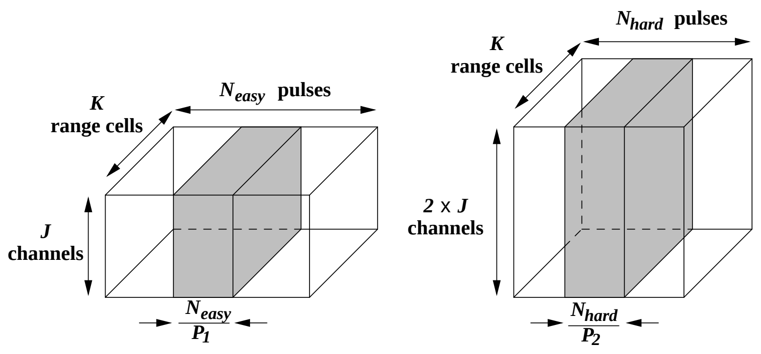

Figure 7. Partitioning strategy for easy and hard weight computation tasks. Data cube is partitioned across dimension N.

to the easy and hard tasks. In Figure 4, P_1 processors are allocated to easy weight computation and P_2 processors to hard weight computation. Since weight vectors are computed for each pulse (Doppler bin), the parallelization in this step involves partitioning of the data along dimension N, that is, each processor in easy weight computation task is responsible for $\frac{N_{easy}}{P_1}$ pulses while each processor in hard weight computation task is responsible for $\frac{N_{hard}}{P_2}$ pulses, as shown in Figure 7.

Notice that the Doppler filter processing and weight computation tasks employ different data partitioning strategies (along different dimensions.) Due to different partitioning strategies, an all-to-all personalized communication scheme is required for data redistribution from the Doppler filter processing task to the weight computation task. That is, each of the P_1 and P_2 processors needs to communicate with all P_0 processors allocated to the Doppler filter processing task to receive CPI data. Since only subsets of the Doppler filter processing task's output are used in the weight computation task, data collection is performed before inter-task communication. Although data collection reduces inter-task communication cost, it also involves data copying from non-contiguous memory space to contiguous buffers. Sometimes the cost of data collection may become extremely large due to hardware limitations (e.g. high cache miss ratio.) When sending data to the beamforming task, the weight vectors have already been partitioned along dimension N which is the same as the data partitioning strategy for the beamforming task. Therefore, no data collection is needed when transferring data to the beamforming task.

5.3 Beamforming

The third step in this pipeline (which is actually the second step for the current CPI because the result of the weight task is only used in the subsequent time step) is beamforming. The inputs of this task are received from both the Doppler filter processing and weight computation tasks, as shown in Figure 4. The easy weight vector received from the easy weight computation task is applied to the easy Doppler bins of the received CPI data while the hard weight vector is applied to the hard Doppler bins. The application of weights to CPI data requires matrix-matrix multiplications on two received data sets. Due to different matrix sizes for the multiplications in the easy and hard beamforming tasks, uneven computational load results. The beamforming task is also divided into easy and hard parts for parallelization purposes. This is because the easy and hard beamforming tasks require different amounts and portions of CPI data, and involve different computational loads. The inputs for the easy beamforming task are two 3-dimensional complex data cubes. One data cube, which is received from the easy weight computation task, is of size $N_{easy} \times M \times J$. The other is from the Doppler filter processing task and its size is $N_{easy} \times J \times K$. A total of N_{easy} matrix-matrix multiplications are performed where each multiplication involves two matrices of size $M \times J$ and $J \times K$, respectively. The hard beamforming task also has two input data cubes which are received from the Doppler filter processing and hard weight computation tasks. The data cube of size $6N_{hard} \times M \times 2J$ is received from the hard weight computation task and the Doppler filtered CPI data cube is of size $N_{hard} \times 2J \times K$. Since range cells are divided into 6 range segments, there are a total of $6N_{hard}$ matrix-matrix multiplications in hard beamforming. The results of the beamforming task are two 3-dimensional complex data cubes of size $N_{easy} \times M \times K$ and $N_{hard} \times M \times K$ corresponding to the easy and hard parts, respectively.

In a manner similar to the weight computation task, parallelization in this step also involves partitioning of data across the N dimension (Doppler bins.) Different sets of processors are allocated to the easy and hard beamforming tasks. Since the cost of matrix multiplications can be determined accurately, the computations are equally divided among the allocated processors for this task. As seen from Figure 4, this task requires data to be communicated from the first as well as the second task. Because data is partitioned along different dimensions, an all-to-all personalized communication is required for data redistribution between the Doppler filter processing and beamforming

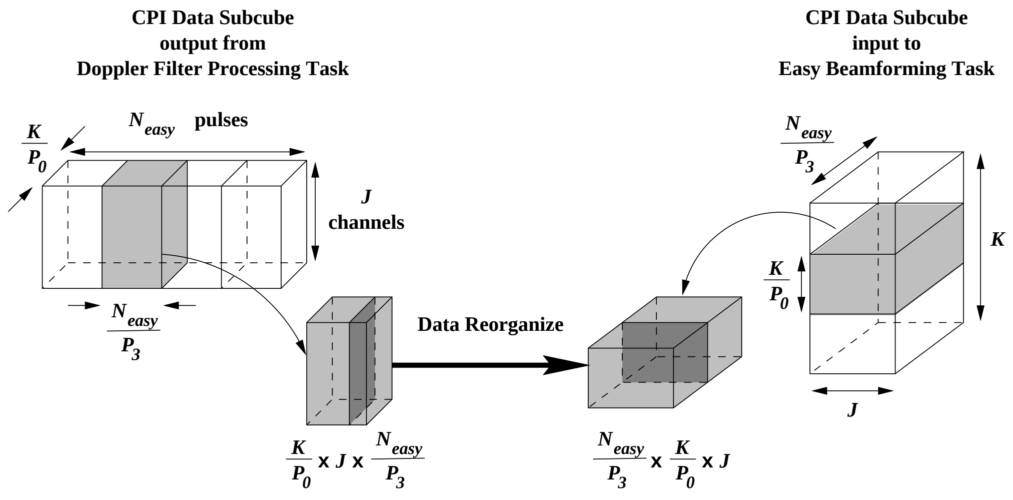

CPI Data Subcube output from Doppler Filter Processing Task
CPI Data Subcube input to Easy Beamforming Task
N_{easy} pulses
$\frac{K}{P_0}$
J channels
$\frac{N_{easy}}{P_3}$
Data Reorganize
$\frac{K}{P_0}$ x J x $\frac{N_{easy}}{P_3}$
$\frac{N_{easy}}{P_3}$ x $\frac{K}{P_0}$ x J
K
J

Figure 8. Data redistribution from Doppler filter processing task to easy beamforming task. CPI data subcube of size $\frac{K}{P_0} \times J \times \frac{N_{easy}}{P_3}$ is reorganized to subcube of size $\frac{N_{easy}}{P_3} \times \frac{K}{P_0} \times J$ before sending from one processor in Doppler filter processing task to another in easy beamforming task.

tasks. The output of the Doppler filter processing task is a data cube of size $K \times 2J \times N$ which is redistributed to the beamforming task after data reorganization in the order of $N \times K \times 2J$. Data reorganization has to be done before the inter-task communication between the two tasks takes place, as shown in Figure 8.

Data reorganization involves data copying from non-contiguous memory space and its cost may become extremely large due to cache misses. For example, two Doppler bins in the same range cell and the same channel are stored in contiguous memory space. After data reorganization, they are $\frac{K}{P_0} \cdot J$ element distance apart. Therefore, if P_0 is small and the size of the CPI data subcube partitioned in each processor is large, then it is quite likely that expensive data reorganization will be needed which becomes a major part of the communication overhead. The algorithms which perform data collection and reorganization are crucial to exploit the available parallelism. Note that receiving data from the weight computation tasks does not involve data reorganization or data collection because they have the same partitioning strategy (along dimension N.)

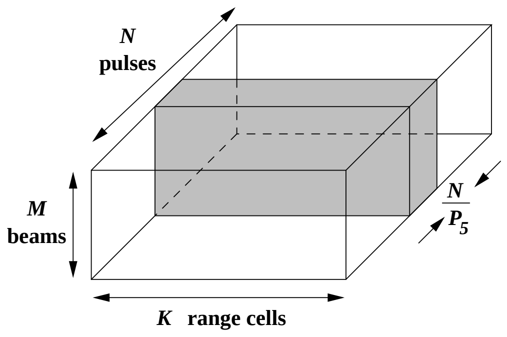

Figure 9. Partitioning strategy for pulse compression task. Data cube is partitioned across dimension N into P_5 processors.

5.4 Pulse Compression

The input to the pulse compression task is a 3-dimensional complex data cube of size $N \times M \times K$, as shown in Figure 9. This data cube consists of two subcubes of size $N_{easy} \times M \times K$ and $N_{hard} \times M \times K$ which are received from the easy and hard beamforming tasks, respectively. Pulse compression involves convolution of the received signal with a replica of the transmit pulse waveform. This is accomplished by first performing K-point FFTs on the two inputs, point-wise multiplication of the intermediate result and then computing the inverse FFT. The output of this step is a 3-dimensional real data cube of size $N \times M \times K$. The parallelization of this step is straightforward and involves the partitioning of the data cube across the N dimension. Each of the FFTs could be performed on an individual processor and, hence, each processor in this task gets an equal amount of computation. Partitioning along the N dimension also results in an efficient accessing mechanism for contiguous memory space when running FFTs. Since both the beamforming and pulse compression tasks use the same data partitioning strategy (along dimension N), no data collection or reorganization is needed prior to communication between these two tasks. After pulse compression, the square of the magnitude of the complex data is computed to move to the real power domain. This cuts the data set size in half and eliminates the computation of the square root.

5.5 CFAR Processing

The input to this task is an $N \times M \times K$ real data cube received from the pulse compression task. The sliding window constant false alarm rate (CFAR) processing compares the value of a test cell at a given range to the average of a set of reference cells around it times a probability of false alarm factor. This step involves summing up a number of range cells on each side of the cell under test, multiplying the sum by a constant, and comparing the product to the value of the cell under test. The output of this task, which appears at the pipeline output, is a list of targets at specified ranges, Doppler frequencies, and look directions. The parallelization strategy for this step is the same as for the pulse compression task. Both tasks partition the data cube along the N dimension. Also, no data collection or reorganization is needed in the pulse compression task before sending data to this task.

6 Software Development and System Platform

All the parallel program development and their integration was performed using ANSI C language and message passing interface (MPI) [24]. This permits easy portability across various platforms which support C language and MPI. Since MPI is becoming a de facto standard for high-performance systems, we believe the software is portable.

The implementation of the STAP application based on our parallel pipeline system model has been done on the Intel Paragon at the Air Force Research Laboratory, Rome, New York. This machine contains 321 compute nodes interconnected in a two-dimensional mesh. The Paragon runs Intel's standard Open Software Foundation (OSF) UNIX operating system. Each compute node consists of three i860 RISC processors which are connected by a system bus and share a 64M byte memory. The speed of an i860 RISC processor is 40 MHz and its peak performance is 100M floating point operations per second. The interconnection network has a message startup time of 35.3 μsec and a data transfer time of 6.53 nsec/byte for point-to-point communication.

In our implementation, a double buffering strategy was used both in the receive and send phases. During the execution loops, this strategy employs two buffers alternatively such that one buffer can be processed during the communication phase while the other buffer is processed during the compute phase. Together with the double buffering implementation, asynchronous send and receive

n	: number of CPIs
inBuf[2]	: input data buffer
outBuf[2]	: output data buffer

```
for $i \leftarrow 0$ to $n - 1$
    $prev \leftarrow (i - 1)$ mod $2$
    $cur \leftarrow i$ mod $2$
    $next \leftarrow (i + 1)$ mod $2$
    $t_0 \leftarrow$ read timer
    post async receives for inBuf[$next$]
    wait for completion of previous receives for inBuf[$cur$]
    data unpacking on inBuf[$cur$]
    $t_1 \leftarrow$ read timer
    computation on inBuf[$cur$] and result in outBuf[$cur$]
    $t_2 \leftarrow$ read timer
    data packing for outgoing message on outBuf[$cur$]
    post async sends for outBuf[$cur$] to next task
    wait for completion of sends for outBuf[$prev$]
    $t_3 \leftarrow$ read timer
```

Figure 10. Implementation of timing computation and communication for each task. A double buffering strategy is used to overlap the communication with the computation. Receive time = $t_1 - t_0$, compute time = $t_2 - t_1$, and send time = $t_3 - t_2$.

calls were employed in order to maximize the overlap of communication and computation. Asynchronous communication means that the program executing the send/receive does not wait until the send/receive is complete. This type of communication is also referred to as non-blocking communication. The other option is synchronous communication which blocks the send/receive operation till the message has been sent/received. The general execution flow and the approach to measure the timing for each part of computation and communication is given in Figure 10. We used MPI timer, MPI_Wtime(), because this function is portable with high resolution.

Table 1. The number of floating point operations for the PRI-staggered post Doppler STAP algorithm to process one CPI data.

Task	number of floating point operations
Doppler filter processing	79,691,776
hard weight computation	197,038,464
easy weight computation	13,851,792
easy beamforming	28,311,552
hard beamforming	44,040,192
pulse compression	38,928,384
CFAR processing	1,690,368
Total	403,552,528

7 Performance Results

We specified the parameters that were used in our experiments as follows:

- range cells (K) = 512,
- channels (J) = 16,
- pulses (N) = 128,
- receive beams (M) = 6,
- easy Doppler bins (N_{easy}) = 72, and
- hard Doppler bins (N_{hard}) = 56.

Given these values of parameters, the total number of floating point operations (flops) required for each CPI data to be processed throughout this STAP algorithm is 403,552,528. Table 1 shows the number of flops required for each task. A total of 25 CPI complex data cubes were generated as inputs to the parallel pipeline system. Each task in the pipeline contains three major parts: receiving data from the previous task, main computation, and sending results to the next task. Performance results are measured separately for these three parts, namely receiving time, computation time, and

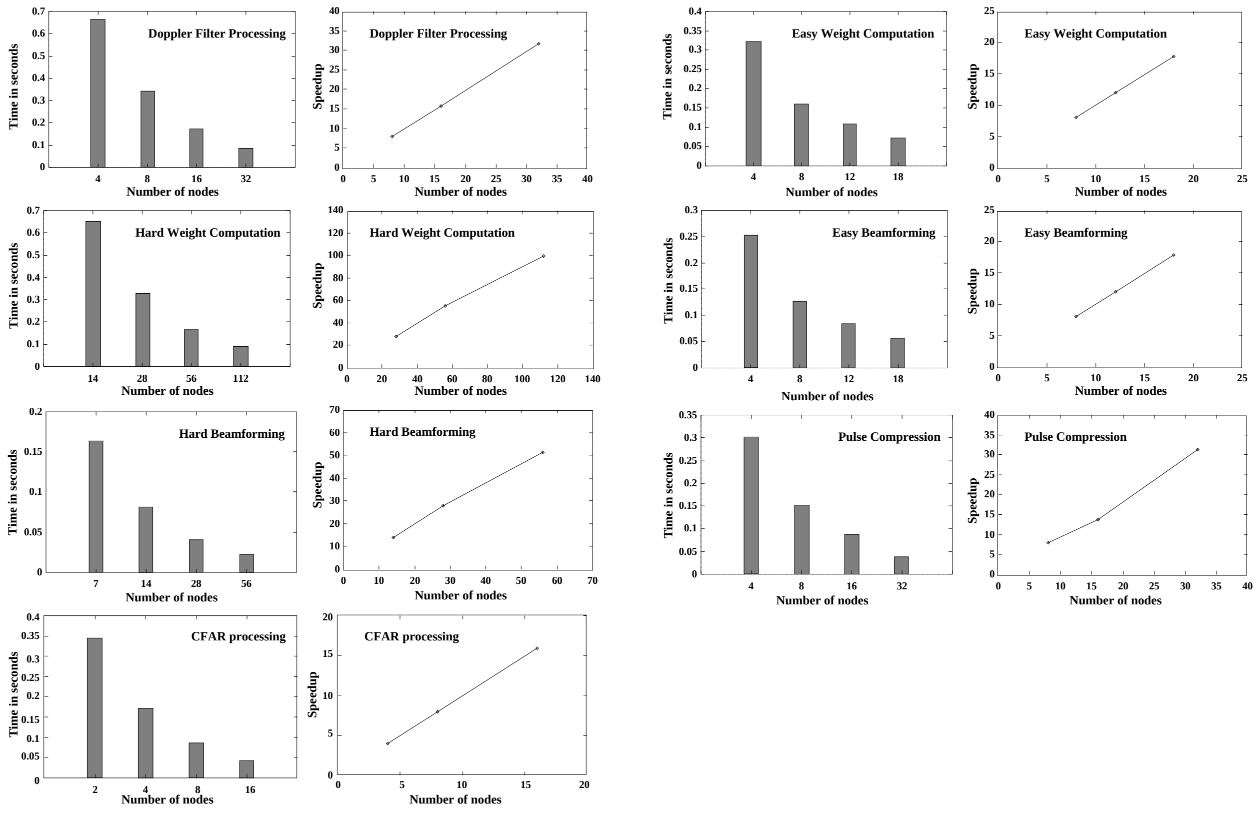

Figure 11. Performance and speedup of computation time as a function of number of compute nodes for all tasks.

sending time. In each task timing results for processing one CPI data were obtained by accumulating the execution time for the middle 20 CPIs and then averaging it. Timing results presented in this paper do not include the effect of the initial setup (first 3 CPIs) and final iterations (last 2 CPIs).

7.1 Computation Costs

The task of computing hard weights is the most computationally demanding task. The Doppler filter processing task is the second most demanding task. Naturally, more compute nodes are assigned to these two tasks in order to obtain a good performance. For each task in the STAP algorithm, parallelization was done by evenly dividing the computational load across the compute nodes assigned. Since there is no intra-task data dependency, no inter-processor communication

Table 2. Timing results of inter-task communication from Doppler filter processing task to its successor tasks. Time in seconds.

		easy weight		hard weight				easy BF		hard BF	
	# nodes	16		56		112		16		16	
		send	recv	send	recv	send	recv	send	recv	send	recv
Doppler filter	8	.1332	.4339	.1332	.3603	.1332	.4441	.1332	.4509	.1332	.4395
	16	.0679	.1780	.0679	.1048	.0679	.1837	.0679	.1955	.0679	.1843
	32	.0340	.0511	.0332	.0034	.0340	.0563	.0340	.0646	.0340	.0519

occurs within any single task in the pipeline. Another way to view this is that intra-task communication is moved to the beginning of each task within the data redistribution step. Figure 11 gives the computation performance results as functions of the numbers of nodes and the corresponding speedup on the AFRL Intel Paragon. For each task, we obtained linear speedups.

7.2 Inter-task Communication

Inter-task communication refers to the communication between the sending and receiving (distinct and parallel) tasks. This communication cost depends on both the processor assignment for each task as well as on the volume and extent of data reorganization. Tables 2 to 6 present the inter-task communication timing results. Each table considers pairs of tasks where the number of compute nodes for both tasks are varied. In some cases timing results shown in the tables contain idle time for waiting for the corresponding task to complete. This happens when the receiving task's computation part completes before the sending task has generated data to send.

From most of the results (Tables 2 to 6) the following important observations can be made. First, when the number of nodes is unbalanced (e.g., sending task has a small number of nodes while the receiving task has a large number of nodes), the communication performance is not very good. Second, as the number of nodes is increased in the sending and receiving tasks, communication scales tremendously. This happens for two reasons. One, each node has less data to reorganize, pack and send and each node has less data to receive; and two, contention at the sending and receiving nodes is reduced. For example, Table 2 shows that when the sending task's number of

Table 3. Timing results of inter-task communication from easy weight computation task to easy beamforming task. Time in seconds.

		easy beamforming			
	# nodes	8		16	
		send	recv	send	recv
easy weight	4	.0005	.1956	.0007	.2570
	8	.0088	.0883	.0004	.0905
	16	.0768	.0807	.0003	.0660

Table 4. Timing results of inter-task communication from hard weight computation task to hard beamforming task. Time in seconds.

		hard beamforming			
	# nodes	8		16	
		send	recv	send	recv
hard weight	28	.0007	.1798	.0007	.2485
	56	.0100	.1468	.0065	.0765
	112	.1824	.1398	.0005	.0543

nodes is increased from 8 to 32, the communication times improve in a superlinear fashion. Thus, it is not sufficient to improve the computation times for such parallel pipelined applications to improve throughput and latency.

In Figure 10 the receiving time for each loop is given by subtracting t_1 from t_0. Since computation has to be performed only after the input data has been received, receiving time may contain the waiting time for the input, shown in line 4. Sending time, $t_3 - t_2$, measures the time containing data packing (collection and reorganization) and posting sending requests. Because of the asynchronous send used in the implementation, the results shown here are the visible sending time and the actual sending action may occur in other portions of the task. Similar to the receiving time, the sending time may also contain the waiting time for the completion of sending requests in the previ-

Table 5. Timing results of inter-task communication from easy and hard beamforming tasks to pulse compression task. Time in seconds.

		pulse compression			
	# nodes	8		16	
		send	recv	send	recv
easy BF	4	.0069	.5016	.0069	.5714
	8	.0036	.1379	.0036	.2090
	16	.0580	.0771	.0022	.0569
		send	recv	send	recv
hard BF	4	.0054	.5016	.0054	.5714
	8	.0029	.1379	.0030	.2090
	16	.1159	.0771	.0017	.0569

Table 6. Timing results of inter-task communication from pulse compression task to CFAR processing task. Time in seconds.

		CFAR processing			
	# nodes	4		8	
		send	recv	send	recv
pulse compr	4	.0099	.3351	.0098	.3348
	8	.0053	.0662	.0051	.1750
	16	.1256	.0435	.0028	.1783

ous loop, shown in line 8. Especially in the cases when two communicating tasks have an uneven partitioned parallel computation load, this effect becomes more apparent. With a large number of nodes, there is tremendous scaling in performance of communicating data as the number of nodes is increased. This is because the amount of processing for communication per node is decreased (as it handles less amount of data), the amount of data per node to be communicated is decreased and the traffic on links going in and out of each node is reduced. This model scales well for both computation and communication.

7.3 Integrated System Performance

Integrated system refers to the evaluation of performance when all the tasks are considered together. Throughput and latency are the two most important measures for performance evaluation in addition to individual task computation time and inter-task communication time. Table 7 gives timing results for three different cases with different node assignments.

In section 5 equations (1) and (2) provide the throughput and latency for one CPI data set. The measured throughput is obtained by placing a timer at the end of the last task and recording the time difference between every loop (that is between two successive completions of the pipeline.) The inverse of this measure provides the throughput. On the other hand, it is more difficult to measure latency because it requires synchronizing clocks at the first and last task's nodes. Thus, to obtain the measured latency, the timing measurement should be made by first reading time at both the first task and last task when the first task is ready to read a new input data. This can be done by sending a signal from the first task to the last task when the first task is ready for reading the new input data. Then the timer for the last task can be started.

In fact, the latency given in equation (2) represents an **upper bound** because the way we time tasks contains the time of waiting for input from the previous task. This waiting time portion overlaps with the computation time in the previous tasks and should be excluded from the latency. Thus, the latency results are conservative values and the real latency is expected to be smaller than this value. However, the latency given from equation (2) indicates the worst-case performance for our implementation. The real latency equation, therefore, becomes

$$real\ \ latency = T_0 + \max(T'_3, T'_4) + T'_5 + T'_6 \tag{3}$$

where T'_i = T_i - idle time at receiving, i = 3, 4, 5, and 6.

Table 8 gives the throughput and latency results for the 3 cases shown in Table 7. From these 3 cases, it is clear that even for the latency and throughput measures we obtain linear speedups from our experiments. Given that this scale up is up to compute 236 nodes (we were limited to these number of nodes due to the size of the machine), we believe these are very good results.

As discussed in section 4, tradeoffs exist between assigning nodes to maximize throughput and to minimize latency, given limited resources. Using two examples, we illustrate how further performance improvements may (or may not) be achieved if few extra nodes are available. We now

Table 7. Performance results for 3 cases with different node assignments. Time in seconds.

case 1: total number of nodes = 236

	# nodes	recv	comp	send	total
Doppler filter	32	.0055	.0874	.0348	.1276
easy weight	16	.0493	.0913	.0003	.1408
hard weight	112	.0555	.0831	.0005	.1390
easy BF	16	.0658	.0708	.0021	.1387
hard BF	28	.0936	.0414	.0010	.1361
pulse compr	16	.0551	.0776	.0028	.1355
CFAR	16	.0910	.0434	-	.1344
throughput	7.2659				
latency	0.3622				

case 2: total number of nodes = 118

	# nodes	recv	comp	send	total
Doppler filter	16	.0110	.1714	.0668	.2492
easy weight	8	.0998	.1636	.0003	.2637
hard weight	56	.0979	.1636	.0005	.2621
easy BF	8	.1302	.1267	.0036	.2605
hard BF	14	.1782	.0822	.0017	.2622
pulse compr	8	.1027	.1543	.0051	.2621
CFAR	8	.1742	.0864	-	.2606
throughput	3.7959				
latency	0.6805				

case 3: total number of nodes = 59

	# nodes	recv	comp	send	total
Doppler filter	8	.0219	.3509	.1296	.5024
easy weight	4	.1796	.3254	.0003	.5053
hard weight	28	.1779	.3265	.0006	.5050
easy BF	4	.2439	.2529	.0068	.5037
hard BF	7	.3370	.1636	.0032	.5039
pulse compr	4	.1806	.3067	.0097	.4970
CFAR	4	.3240	.1723	-	.4963
throughput	1.9898				
latency	1.3530				

Table 8. Throughput and latency for the 3 cases in Table 7. Real results are obtained from the experiments while equation results are obtained from applying individual tasks' timing to equations (1) and (2). The unit of throughput is number of CPIs per second. The unit of latency is second.

# of nodes		236	118	59
throughput	equation	7.1019	3.7919	1.9791
	real	7.2659	3.7959	1.9898
latency	equation	0.5362	1.0346	1.9996
	real	0.3622	0.6805	1.3530

Table 9. Performance results for adding 4 more nodes to Doppler filter processing task to case 2 in Table 7. Time in seconds.

total number of nodes = 122

	# nodes	recv	comp	send	total
Doppler filter	20	.0090	.1395	.0540	.2024
easy weight	8	.0519	.1633	.0003	.2155
hard weight	56	.0486	.1644	.0005	.2135
easy BF	8	.0815	.1272	.0037	.2124
hard BF	14	.1232	.0823	.0018	.2073
pulse compr	8	.0519	.1543	.0051	.2113
CFAR	8	.1240	.0864	-	.2105
throughput	5.0213				
latency	0.5498				

take case 2 from Table 7 as an example and add some extra nodes to tasks to analyze its affect to the throughput and latency. Suppose that case 2 has fulfilled the minimum throughput requirement and more nodes can be added. Table 9 shows that adding 4 more nodes to the Doppler filter processing task not only increases the throughput but also reduces the latency. This is because the communication amount for each send and receive between the Doppler filter processing task to

Table 10. Performance results for adding 16 more nodes to pulse compression and CFAR processing tasks to the case in Table 9. Time in seconds.

total number of nodes = 138

	# nodes	recv	comp	send	total
Doppler filter	20	.0091	.1395	.0541	.2027
easy weight	8	.0516	.1633	.0003	.2152
hard weight	56	.0488	.1644	.0005	.2137
easy BF	8	.0819	.1273	.0037	.2129
hard BF	14	.1301	.0823	.0018	.2142
pulse compr	16	.1337	.0775	.0028	.2140
CFAR	16	.1701	.0434	-	.2135
throughput	4.9052				
latency	0.4247				

weight computation and to beamforming tasks is reduced (Table 9). So, clearly, adding nodes to one task not only affects that task's performance but has a measurable effect on the performance of other tasks. By increasing the number of nodes 3%, the improvement in throughput is 32% and in latency is 19%. *Such effects are very difficult to capture in purely theoretical models because of the secondary effects.*

Since the parallel computation load may be different among tasks, bottleneck problems arise when some tasks in the pipeline do not have the proper numbers of nodes assigned. If the number of nodes assigned to one task with a heavy work load is not enough to catch up the input data rate, this task becomes a bottleneck in the pipeline system. Hence, it is important to maintain approximately the same computation time among tasks in the pipeline system to maximize the throughput and, also, achieve higher processor utilization. One bottleneck task can be seen when its computation time is relatively much larger than the rest of the tasks. The entire system's performance degrades because the rest of the tasks have to wait for the bottleneck task's completion to send/receive data to/from it no matter how many more nodes assigned to them and how fast they can complete their jobs. Therefore, poor task scheduling and processor assignment will cause a significant portion of idle time in the resulted communication costs. In Table 10 we added a total of 16 more nodes to the pulse compression and CFAR processing tasks to the case in Table 9. Comparing to case 2 in Table 7, we can see that the throughput increased. However, the throughput did not improve compared to the results in Table 9, even though this assignment has 16 more nodes. In this case, the weight tasks are the bottleneck tasks because their computation costs are relatively higher than other tasks. We can see that the receiving time of the rest of the tasks are much larger than their computation time. A significant portion of idle time waiting for the completion of weight tasks is in the receiving time. On the other hand, we observe 23% improvement in the latency. This is because the computation time is reduced in the last two tasks with more nodes assigned. From equation (3), the execution time of these two tasks, T'_5 and T'_6, decreases and, therefore, the latency is reduced.

8 Conclusions

In this paper we presented performance results for a PRI-staggered post-Doppler STAP algorithm implementation on the Intel Paragon machine at the Air Force Research Laboratory, Rome, New York. The results indicate that our approach of parallel pipelined implementation scales well both in terms of communication and computation. For the integrated pipeline system, the throughput and latency also demonstrate the linear scalability of our design. Linear speedups were obtained for up to 236 compute nodes. When more than 236 nodes are used, the speedup curves for the results of throughput and latency may saturate. This is because the communication costs will become significant with respect to the computation costs.

Almost all radar applications have real-time constraints. Hence, a well designed system should be able to handle any changes in the requirements on the response time by dynamically allocating or re-allocating processors among tasks. Our design and implementation not only shows tradeoffs in parallelization, processor assignment, and various overheads in inter and intra-task communication etc., but it also shows that accurate performance measurement of these systems is very important. Consideration of issues such as cache performance when data is packed and unpacked, and impact of the parallelization and processor assignment for one task on another task are crucial. This is normally not easily captured in theoretical models. In the future we plan to incorporate further optimizations including multi-threading, multiple pipelines and multiple processors on each compute node.

9 Acknowledgments

This work was supported by Air Force Materiel Command under contract F30602-97-C-0026. We acknowledge the use of the Intel Paragon at Caltech for the initial development.

Appendix A: Space-Time Adaptive Processing with Mainbeam Constraint

The space-time adaptive processing problem can be formulated as a least squares minimization of the clutter response. This approach is desirable from a computational standpoint, as it is not necessary to produce an estimate of the clutter covariance matrix, which is an order $\boldsymbol{n}^3$ operation. In the least squares approach, a matrix $\boldsymbol{M}$ is constructed from snapshots of the array data after Doppler processing, and a weight vector $\boldsymbol{w}$ is computed which minimizes the norm of the product vector $\boldsymbol{M}\boldsymbol{w}$. The snapshots are samples of data from each array element taken at range cells adjacent to the test cell, and also from multiple coherent processing intervals (CPI's) which are decorrelated across time. Typically a beam constraint, such as a requirement for unit response in the direction of the desired target, is added to rule out the trivial solution, $\boldsymbol{w} = \boldsymbol{0}$. As illustrated in Figure 12, the weight vector is computed by multiplying the pseudoinverse of $\boldsymbol{M}$ times a unit vector.

$$\boldsymbol{M} = \begin{bmatrix} \text{data vector } \boldsymbol{1} \\ \text{data vector } \boldsymbol{2} \\ \vdots \\ \text{data vector } \boldsymbol{n} \\ \boldsymbol{w}_s^{\boldsymbol{H}} \end{bmatrix}$$

$\boldsymbol{w}$ = column vector of element weights

$\boldsymbol{w}_s$ = steering vector (column)

Find $\boldsymbol{w}$ = least square error solutionof : $\boldsymbol{M}\,\boldsymbol{w} = [\,0\ 0\ \ldots\ 0\ 1]^{\boldsymbol{T}}$

Figure 12. Conventional least squares processing.

While assuring a nonzero solution for the weights, the conventional beam constraint placed on the least squares problem as formulated above often produces an adapted pattern with a highly distorted main beam with a peak response far removed from the target of interest. The algorithm that was formulated and implemented here is a constrained version of the least squares problem. Given a steering vector $\boldsymbol{w}_s$ we seek a weight vector $\boldsymbol{w}$ that minimizes the clutter response while

$$\boldsymbol{M} = \begin{bmatrix} \text{data vector } \boldsymbol{1} \\ \text{data vector } \boldsymbol{2} \\ \vdots \\ \text{data vector } \boldsymbol{n} \\ \text{Identity Matrix } * \ \boldsymbol{k} \end{bmatrix}$$

$\boldsymbol{w}$ = column vector of element weights

$\boldsymbol{w_s}$ = steering vector (column)

$\boldsymbol{k}$ = beam constraint weight

Find $\boldsymbol{w}$ = least square error solutionof : $\boldsymbol{M\,w} = [\,0\;0\;.\,.\,.\;0\;\;\boldsymbol{w_s^H}\,]^{\boldsymbol{H}}$

Figure 13. Beam constrained least squares processing.

maintaining a close similarity between $\boldsymbol{w}$ and $\boldsymbol{w_s}$. This condition is specified by augmenting the data matrix $\boldsymbol{M}$ with an identity matrix as depicted in Figure 13. The product of the identity matrix and the solution vector $\boldsymbol{w}$ is set to a scalar multiple of the steering vector $\boldsymbol{w_s}$. The least squares solution is a compromise between clutter rejection and preservation of main beam shape. In practice, only slight modifications of the weight vector are required to move spatial nulls into the clutter region, for clutter returns that are outside of the main beam. Thus, preservation of main beam shape requires only a slight reduction of clutter rejection performance, and is often offset by an increase in array gain on the desired target. As shown in Figure 13, the preservation of main beam shape is controlled by scalar $\boldsymbol{k}$. The choice of $\boldsymbol{k}$ directs the least squares solution for $\boldsymbol{w}$ to adhere more closely to the steering vector when $\boldsymbol{k}$ is large, and emphasize clutter cancellation at the expense of beam shape when $\boldsymbol{k}$ is small. Since $\boldsymbol{k}$ is variable depending on operating requirements, we normalize the resulting weight vector to unit length.

There is a computational advantage of the constrained technique of Figure 13 over that of Figure 12 for systems that utilize multiple beam steering. Since the steering vector $\boldsymbol{w_s}$ appears only on the right side of the equation, and matrix $\boldsymbol{M}$ is independent of the main beam pointing angle, the QR factorization of $\boldsymbol{M}$ needs be performed only once for a given data set. Multiple weight vectors can be computed for different steering vector choices by multiplying the same matrix pseudoinverse or QR factorization by several choices of constraint vectors.

Appendix B: Matlab Version of RT-MCARM processing Algorithm

```
function [detections] = process_CPI(CPI_data, N)
    % N is the CPI number

    num_channels             = 16;
    num_range                = 512;
    num_pulses               = 128;
    num_doppler              = num_pulses;
    numHardDop               = 56;
    stagger                  = 3;    % PRI-stagger pulses
    BeamConstraintWt         = 0.5;
    FreqConstraintWt         = 0.5;
    DopplerWindow            = hanning(num_pulses-stagger);
    range_Segment_Boundaries= [0 75 150 225 300 375 512];

    % Doppler Filter Processing
    doppler_data = rawToFFT(CPI_data,DopplerWindow,stagger);

    % Easy Weight Computation and Beamforming
    beamformed_data(numHardDop/2+1:num_doppler-numHardDop/2) = easy_wts.' * doppler_data;
    easy_wts = zeros(num_doppler,num_channels,num_beams);
    for idop = numHardDop/2+1 : num_doppler - numHardDop/2,
        [easy_wts(idop,:,:), previous_doppler_data(idop,:,:)] = computeEasyWts(idop,BeamConstraintWt,    ...
            Steering_vectors,previous_doppler_data(idop,:,:),doppler_data(idop,:,:));
    end;

    % Hard Weight Computation and Beamforming
    for rangeSeg = 1:num_range_segments,
        startR = range_Segment_Boundaries(rangeSeg)+1;
        endR = range_Segment_Boundaries(rangeSeg+1);

        beamformed_data(1:numHardDop/2,:,startR:endR) = hard_wts(rangeSeg,1:numHardDop/2,:,:).' *     ...
            doppler_data(1:numHardDop/2,:,startR:endR);
        beamformed_data(num_doppler-numHardDop/2+1:num_doppler,:,startR:endR) =                       ...
            hard_wts(rangeSeg,num_doppler-numHardDop/2+1:num_doppler,:,:).' *                        ...
            doppler_data(num_doppler-numHardDop/2+1:num_doppler,:,startR:endR);

        hard_wts = zeros(num_range_segments,num_doppler,num_channels,num_beams);
        for idop = 1:numHardDop/2,
            [wts(rangeSeg,idop,:,:), new_r(idop,:,:)] = computeRecurHardWts(idop,startR,endR,         ...
                FreqConstraintWt,BeamConstraintWt,Steering_Vectors,doppler_data(idop,:,:),           ...
                new_r(idop,:,:),stagger);
        end; % idop
        for idop = num_doppler-numHardDop/2+1:num_doppler,
            [wts(rangeSeg,idop,:,:), new_r(idop,:,:)] = computeRecurHardWts(idop,startR,endR,         ...
                FreqConstraintWt,BeamConstraintWt,Steering_Vectors,doppler_data(idop,:,:),           ...
                new_r(idop,:,:),stagger);
        end; % idop
    end; % range_segments

    % Pulse Compression and CFAR processing
```

```
        pulsecompression = pulseCompression(beamformed,pc_filter_freq);
        detections        = CFAR(pulsecompression);
end; % function process_CPI

function [Doppler_data] = rawToFFT(CPI_data,window,stagger)
        % input: CPI_data(num_pulses,num_range,num_channels)
        % output Doppler_data(num_doppler,num_channels,num_range)

        Doppler_data = zeros(num_doppler,num_channel,num_range);

        padded_CPI_data(1:num_pulses-stagger,:,:) = CPI_data(1:num_pulses-stagger,:,:) .* window);
        padded_CPI_data(num_pulses-stagger+1:num_pulses,:,:) = zeros(stagger,num_channels,num_range);
        Doppler_data(1:num_doppler,:,:) = fft_pulses(padded_CPI_data);

        padded_CPI_data(stagger+1:num_pulses,:,:) = CPI_data(1:num_pulses-stagger,:,:) .* window);
        padded_CPI_data(1:stagger:num_pulses,:,:) = zeros(stagger,num_channels,num_range);
        Doppler_data(num_doppler+1:2*num_doppler,:,:) = fft_pulses(padded_CPI_data);
end; % function rawToFFT

function [wts, updated_doppler_data] = computeEasyWts(doppler,diagWts, Steering_vectors,              ...
        prev_doppler_data,new_doppler_data)
        % computes adaptive weights directly for the easy doppler bins from data from three previous CPIs

        % shift data from previous two CPIs N-1 and N-2 up, overwriting data from CPI N-3
        updated_doppler_data(1:Total_easy_Samples * 2/3,:) =                                           ...
                prev_doppler_data(Total_easy_Samples * 1/3:Total_easy_Samples,:);

        updated_doppler_data(Total_easy_Samples * 2/3,Total_easy_Samples,:) =                          ...
                Select_Range_Samples(Total_easy_Samples * 1/3,new_doppler_data);

        avg = average(updated_doppler_data) * diagWts ;

        for beam=1:num_beams,
                work = updated_doppler_data;
                work(updated_doppler_data+1:updated_doppler_data+num_channels,:) = avg * eye(num_channels);

                rhs = zeros(updated_doppler_data+num_channels,1);
                rhs(updated_doppler_data+1:updated_doppler_data+num_channels,1) = Steering_vectors(:,beam);

                wts(:,beam) = work\rhs;
                wts(:,beam) = wts(:,beam)/(sqrt(wts(:,beam)'* wts(:,beam)));
        end;
end; % function computeEasyWts

function [wts, new_r] = computeRecurHardWts(doppler,startRangeSeg,endRangeSeg,spatialWt,freqWt,        ...
        Steering_vectors,doppler_data,old_r,stagger, CPI_Num)
        % computes adaptive weights recursively for the hard doppler bins.

        forgettingFactor = 0.6;
        qr_x = zeros(2*num_channels + num_hard_samples,2*num_channels);
        qr_x(1:2*num_channels,:) = forgettingFactor * old_r;
        qr_x(2*num_channels+1:2*num_channels+num_hard_samples,:) =                                     ...
                Select_Range_Samples(num_hard_samples,doppler_data);
        avg = average(qr_x);
        half_channels = num_channels/2;
        if (CPI_Num mod 2 = 1) then colOffset = 0;
        else colOffset = half_channels;
        end;
        % constrain half of the columns
        qr_x(num_hard_samples + 2*num_channels+1,1+colOffset:half_channels+colOffset) =                    ...
                [avg * eye(half_channels)]; % spatial constraints
        qr_x(num_hard_samples + 2*num_channels+1,
                num_channels+1+colOffset:num_channels+half_channels+colOffset) =                           ...
                [avg * eye(half_channels) * exp(-j * 2 * pi * (doppler-1) * stagger / num_doppler)];
        [q new_r] = qr(qr_x(1:num_hard_samples + 2*num_channels + half_channels,:),0);

        for beam=1:num_beams,
                work = new_r;
                % freq constraints scaled by e(-jk/n)
                work(2*num_channels+1:3*num_channels,1:num_channels) = [avg * eye(num_channels)];

                rhs = zeros(3*num_channels,1);
                rhs(2*num_channels+1:3*num_channels,1) = Steering_vectors(:,beam);

                [q2 r2] = qr([work rhs],0);
                matrhs(:,beam) = r2(1:2*num_channels,2*num_channels+1);

                wts(:,beam) = work\rhs;
                wts(:,beam) = wts(:,beam)/(sqrt(wts(:,beam)'* wts(:,beam)));
        end;
end; % function computeRecurHardWts
```

References

[1] M. Linderman and R. Linderman, “Real-Time STAP Demonstration on an Embedded High Performance Computer,” *IEEE AES Systems Magazine*, pp. 15–21, Mar. 1998.

[2] R. Brown and R. Linderman, “Algorithm Development for an Airborne Real-Time STAP Demonstration,” in *Proceedings of the IEEE National Radar Conference*, 1997.

[3] M. Little and W. Berry, “Real-Time Multi-Channel Airborne Radar Measurements,” in *Proceedings of the IEEE National Radar Conference*, 1997.

[4] V. Kumar, A. Grama, A. Gupta, and G. Karypis, *Introduction to Parallel Computing: Design and Analysis of Algorithms,* Benjamin-Cummings, 1994.

[5] G. Fox, M. Johnson, G. Lyzenga, S. Otto, J. Salmon, and D. Walker, *Solving Problems on Concurrent Processors,* Prentice-Hall, Englewood Cliffs, NJ, 1990.

[6] K. Hwang, *Advanced Computer Architecture: Parallelism, Scalability, Programmability*, McGraw-Hill, Inc., 1993.

[7] G. Golub and J. Ortega, *Scientific Computing: An Introduction with Parallel Computing*, Academic Press, Boston, MA, 1993.

[8] C. Xavier and S. Iyengar, *Introduction to Parallel Algorithms,* John Wiley & Sons, Inc., 1998.

[9] J. Lebak, R. Durie, and A. Bojanczyk, “Toward A Portable Parallel Library for Space-Time Adaptive Methods,” Tech. Rep. CTC96TR242, Cornell Theory Center, June 1996.

[10] S. Olszanskyj, J. Lebak, and A. Bojanczyk, “Parallel Algorithms for Space-Time Adaptive Processing,” *International Parallel Processing Symposium*, pp. 77–81, Apr. 1995.

[11] Y. Lim and V. Prasanna, “Scalable Portable Implementations of Space-Time Adaptive Processing,” in *Proceedings of the 10th International Conference on High Performance Computing*, June 1996.

[12] P. Bhat, Y.Lim, and V. Prasanna, "Issues in using Heterogeneous HPC Systems for Embedded Real Time Signal Processing Applications," in *Proceedings of the 2nd International Workshop on Real-Time Computing Systems and Applications*, Oct. 1995.

[13] M. Lee and V. Prasanna, "High Throughput-Rate Parallel Algorithms for Space Time Adaptive Processing," *2nd International Workshop on Embedded Systems and Applications*, Apr. 1997.

[14] D. Martinez, "Application of Parallel Processors to Real-Time Sensor Array Processing," *International Parallel Processing Symposium*, Apr. 1999.

[15] K. Cain, J. Torres, and R. Williams, "RT_STAP: Real-Time Space-Time Adaptive Processing Benchmark," Tech. Rep. 96B0000021, MITRE Corporation, Feb. 1997.

[16] C. Brown, M. Flanzbaum, R. Games, and J. Ramsdell, "Real-Time Embedded High Performance Computing: Application Benchmarks," Tech. Rep. MTR94B145, MITRE Corporation, Oct. 1994.

[17] A. Choudhary and J. Patel, *Parallel Architectures and Parallel Algorithms for Integrated Vision Systems*, Kluwer Academic Publishers, Boston, MA, 1990.

[18] A. Choudhary and R. Ponnusamy, "Run-Time Data Decomposition for Parallel Implementation of Image Processing and Computer Vision Tasks," *Journal of Concurrency, Practice and Experience*, vol. 4, no. 4, pp. 313–334, June 1992.

[19] A. Choudhary and R. Ponnusamy, "Parallel Implementation and Evaluation of a Motion Estimation System Algorithm using Several Data Decomposition Strategies," *Journal of Parallel and Distributed Computing*, vol. 14, pp. 50–65, January 1992.

[20] R. Thakur, A. Choudhary, and J. Ramanujam, "Efficient Algorithms for Array Redistribution," *IEEE Trans. on Parallel and Distributed Systems*, vol. 6, no. 7, pp. 587–594, June 1996.

[21] M. Berger and S. Bokhari, "A Partitioning Strategy for Nonuniform Problems on Multiprocessors," *IEEE Trans. on Computers*, vol. 36, no. 5, pp. 570–580, May 1987.

[22] F. Berman and L. Snyder, "On Mapping Parallel Algorithms into Parallel Architectures," *Journal of Parallel and Distributed Computing*, vol. 4, pp. 439–458, 1987.

[23] A. Choudhary, B. Narahari, D. Nicol, and R. Simha, "Optimal Processor Assignment for Pipeline Computations," *IEEE Trans. on Parallel and Distributed Systems*, April 1994.

[24] M. Snir and et. al., *MPI The Complete Reference,* The MIT Press, 1995.